ELSEVIER

Materials Science and Engineering A 483–484 (2008) 402–405

MATERIALS SCIENCE & ENGINEERING A

www.elsevier.com/locate/msea

Three-dimensional shape of the early stages of fatigue cracks nucleated in nodular cast iron

C. Verdu *, J. Adrien, J.Y. Buffière

GEMPPM, UMR 5510, INSA de Lyon, 20 Avenue Albert Einstein, 69621 Villeurbanne Cedex, France

Received 6 June 2006; received in revised form 29 September 2006; accepted 29 September 2006

Abstract

High resolution synchrotron X-ray tomography has been used to obtain three-dimensional (3D) images of the early stages of fatigue crack nucleation in a nodular cast iron. Microcracks were observed to initiate at casting defects (microshrinkage) and graphite nodules. The 3D observations have shown that the microcracks form in the material ligament comprised between the specimen surface and the defect. The probability of a defect to initiate a crack was correlated with the size of the defect and its position with respect to the surface. This correlation has been explained on the basis of local stress concentrations in the vicinity of the defect. The 3D observations of samples submitted to different fatigue cycles revealed that a large part of the fatigue life consisted in the progressive fracture of the ligament. The majority of the observed cracks stopped after this fracture process and, therefore, their size did not exceed the initiating defect size even if the crack seemed larger than the defect on the optical surface observations. Only few microcracks, nucleated on the largest defects, continued to grow with short-crack behaviour.
© 2007 Elsevier B.V. All rights reserved.

Keywords: Tomography; Fatigue; Crack initiation; Nodular cast iron; 3D crack shape

1. Introduction

In cast materials, the fatigue life is often controlled by the growth of cracks initiated from inclusions, nodules or other metallurgical defects such as shrinkage cavities [1–7]. Such fatigue cracks are frequently observed early in the fatigue life and consequently crack initiation stage is considered as a negligible part of the whole fatigue life. Moreover, it is often observed that these first microcracks stop during a large part of the fatigue life and most of them remain non-propagating until failure. Because of their very small size, these cracks have a strong three-dimentional character. However, studies of short cracks are generally restricted to surface observations which provide no information about the three-dimensional (3D) shape of cracks. Very few authors [1] studied this 3D aspect of the crack initiation.

High-resolution X-ray tomography is a technique that can be used to visualise the internal structure of materials [8]. Detailed information on the development of short crack shape and crack path in a cast iron has been obtained with this technique [9].

The objective of this study is to observe the early stages of fatigue crack nuclation by X-ray tomography of miniature fatigue specimens and to develop a quantitative analysis from the 3D data.

2. Material and experimental procedure

2.1. Material

The material used in this study was a ferritic ductile cast iron for which the microstructure and the mechanical behaviour had been studied in previous works [3,10]. The chemical composition (by weight) is 3.65%C, 3.2%Si, 0.04%Mg, <0.1%Mn, <0.005%S, 0.02%P. It was cast in chill-block type moulds in order to obtain an as cast spheroidal graphite cast iron of good quality (mimimum of shrinkage cavities). Few microshinkage cavities and some pores remained in the cell joints and zones of final solidification, but they were small from a few micrometers to about a hundred micrometers. The average size and the volume fraction of graphite spheroids were 50 μm and 14% respectively. For a detailed description of the mate-

* Corresponding author. Tel.: +33 472 438055; fax: +33 472 438539.
E-mail address: catherine.verdu@insa-lyon.fr (C. Verdu).

0921-5093/$ – see front matter © 2007 Elsevier B.V. All rights reserved.
doi:10.1016/j.msea.2006.09.178

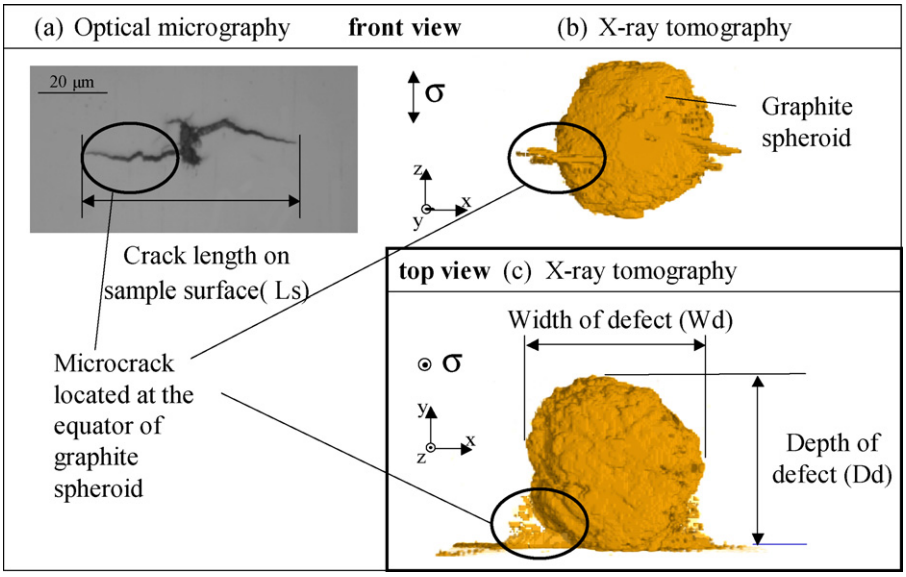

Fig. 1. Example of data obtained by combining surface observations by optical microscopy and X-ray tomography. (a) Surface observation of microcrack located at a graphite spheroid, (b) same view as (a) by X-ray tomography and (c) top and view by X-ray tomography.

rial microstructure and mechanical behaviour see references [3,10].

2.2. Fatigue tests

The in situ tomographic experiments were performed at the European Synchrotron Radiation Facility (ESRF) on the high-resolution tomographic beam-line (ID19). Miniature smooth fatigue specimens with a square cross-section of 0.5 mm × 0.5 mm were specially designed for the experiments. Their size is linked to the rather low X-ray energy (30 kV) used in order to maintain a minimum transmission of the X-ray beam and a spatial resolution of the reconstructed images in the micrometer range. The distance between the sample and the camera was 40 mm in order to obtain phase contrast providing enhanced microcracks detection. 1200 radiographs of the sample were recorded for a 180° rotation and used to reconstruct the 3D volumes. The VGStudio Max software was used for 3D visualisation of the data.

Tensile–tensile fatigue tests were carried out with a stress ratio of 0.1 and a frequency of 5 Hz, using a specially portable fatigue machine providing in situ imaging of cracks.

The maximum applied stress of 400 MPa was determined by previous experiments in order to obtain number of cycles for failure lower than one million cycles. Two samples were tested to 40,000 and 50,000 cycles in order to study the early stages of crack initiation and two other samples to 198,000 and 215,800 cycles to study the growth stage.

Fig. 1 shows an example of data obtained by combining surface observations by optical microscopy and X-ray tomography. For each microcrack, the crack length was measured on the specimen surface. The real size (width) and the location (depth) of the defects were obtained from the 3D reconstructed images.

3. Results and discussion

3.1. Crack initiation

As expected, for uniaxial loading, microcraks were observed at the equator of the casting defects (microshrinkage) and graphite nodules. X-ray tomography confirmed that microcracks were nucleated only on defects located at or near the sample surface (distance between the defect and the surface lower than 10 µm). No microcrack was observed in the bulk.

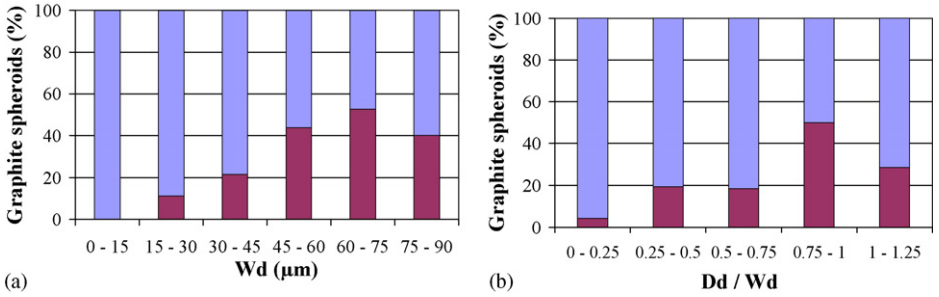

Fig. 2. (a) Defect size dependence of the initiating spheroids fraction. (b) Variation of the fraction of initiating defects with the ratio of the defect depth with the defect width (Dd/Wd).

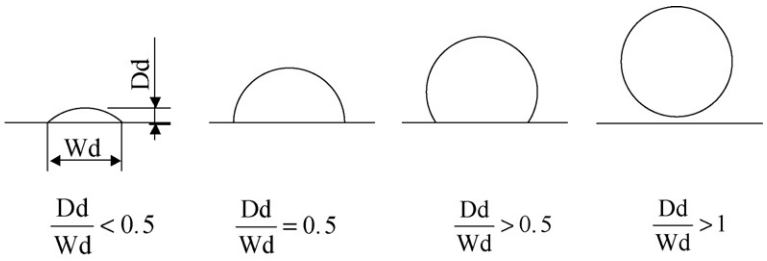

Fig. 3. Schematic illustration of the location of defect with respect to the sample surface versus ratio of the defect depth with the defect width (Dd/Wd).

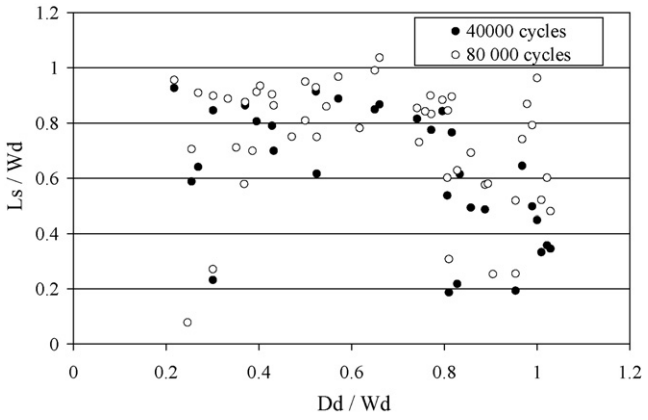

Fig. 4. Size of microcracks in relation with defects characteristics—Ls/Wd ratio as a function of Dd/Wd after 40,000 cycles and 80,000 cycles.

From an experimental point of view, as it is well known [1–7], the 3D observations showed that the probability of a defect to initiate a crack was correlated with the size of the defect (Fig. 2a) but also with its location with respect to the surface sample (Fig. 2b). The ratio Dd/Wd (see Figs. 1 and 3 for a definition of the parameters) was used to characterize the defect position. It should be noted that Dd/Wd = 1 corresponds to a defect that just touches the surface, wheras the case Dd/Wd = 0.5 represents a defect cut in the middle by surface (Fig. 3).

The maximum fraction of initiated defect was obtained for $0.75 < Dd/Wd < 1$ (Fig. 2b). Morever, the most critical defects were the biggest located just under the sample surface.

From a theorical point of view, previous studies [3,10] showed by FE analysis that the von Mises stress was maximal in the equatorial plan of defect. This result can explain why nuclation of microcrack occurs at the defect equator but not why it occurs on the bigger defects. As a matter of fact, 3D microtomographic observations showed that the bigger defect size,the less spherical shape and the less smooth the surface. Moreover, it is well known that local stresses are minimal with a spherical geometry and increase with another geometry [11]. Another FE analysis [12] concluded that in the case of spherical cavities, strain localization occured in the ligament of material between the cavity and the free surface. This strain

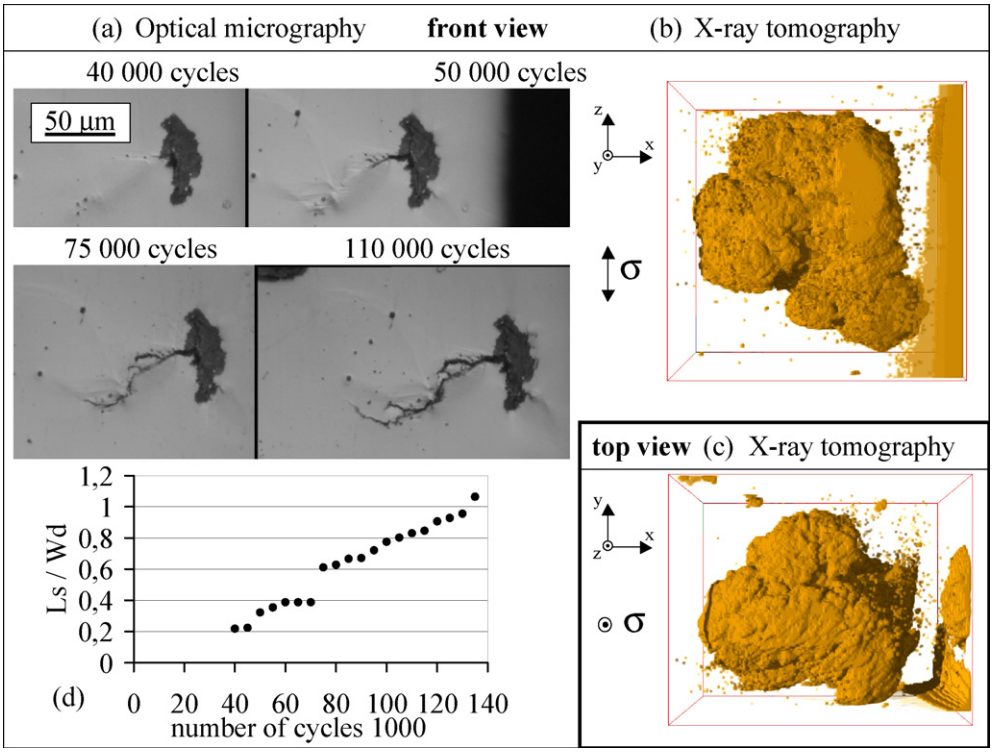

Fig. 5. Growth of a crack initiated on a defect mainly underneath the surface (Dd/Wd = 0.83). (a) Optical micrographies at different numbers of cycles, (b) same view as (a) by X-ray tomography at 40,000 cycles, (c) top view by X-ray tomography and (d) evolution of the ratio Ls/Wd with the number of cycles.

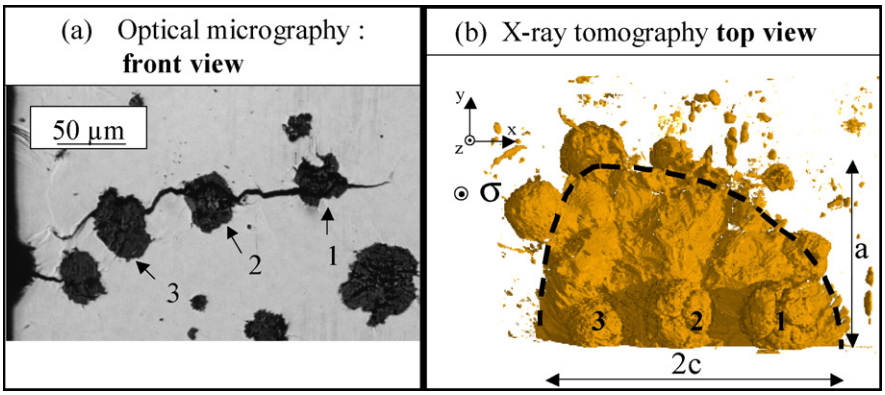

Fig. 6. Crack initiated on a spheroids cluster. The distance between two spheroids (d_{1-2} = 15 µm, d_{2-3} = 7 µm) is less than the average distance ($d_{average}$ = 30 µm). (a) Surface observation and (b) top view by X-ray tomography—the shape of the crack in the bulk is approximately semi-elliptical (dashed line).

localization was most severe for cavities just touching the surface.

3.2. 3D shape of crack and crack growth

Tomography observations allowed to study the 3D shape of microcracks initiated on nodules and microshrinkages. Fig. 1 shows that the cracks formed initially inside the ligament of matrix between the surface and the defect whatever the type of defect may be (spheroid or porosity). A quantitative analysis was carried out by considering the ratio of the crack length Ls on surface and width of defect Wd. It appears in Fig. 4 that after 40,000 cycles Ls/Wd remained less than one. Morever for the defects whose just touched the surface, this ratio could be very small. It suggests that any crack did not propagate beyond the defect as already observed [13].

After 3D tomography characterization, the sample was tested again and optical observations were performed at regular intervals of 5000–135,000 cycles in order to measure the crack length on surface sample. As expected, the number of microcracks increased and some of them propagated during cycling (Fig. 4). Fig. 5 shows the growth of one microcrack which seemed larger than the defect after 75,000 cycles. In fact, the ratio Ls/Wd remained less than one to 130,000 cycles. This behaviour was the same for all microcracks (except one) that presented also a ratio Ls/Wd less than one after 80,000 cycles (Fig. 4). After 100,000 cycles, most of the cracks stopped and became non-propagating.

After 100,000 cycles only few of the previous microcracks reached a ratio Ls/Wd more than one and continued to grow with short crack behaviour. The defects which initiated such short cracks presented a size larger than 80 µm or were spheroids clusters (Fig. 6). In this case, crack shape became approximately semi-elliptical with an aspect ratio a/c equal to 1.15 (a being the crack size in the bulk and $2c$ the crack size at the surface).

4. Conclusion

High resolution synchrotron X-ray tomography was used to study the early stages of fatigue crack nucleation and growth.

3D observations indicated that both the defect size and the defect location in the vicinity of the sample surface control the crack nucleation and revealed that a large part of the fatigue life consisted in the progressive fracture of the ligament of material between the surface sample and the defect.

Most of the studied cracks stopped after their length reached the initiating defect size. Only microcracks initiated on the largest defects or defect clusters continued to grow with short crack behaviour. In this last case, crack shape became semi-elliptical.

Acknowledgements

The financial and technical support of CTIF (Development centre for materials forming industries) for this study is gratefully acknowledged. The authors are grateful to the ID19 staff.

References

[1] P. Clement, J.P. Angeli, A. Pineau, Fatigue Eng. Mater. Struct. 7 (1984) 251–265.
[2] T. Palin-Luc, S. Lassere, J.Y. Berard, Fatigue Fract. Eng. Mater. Struct. 21 (1998) 191–200.
[3] J.P. Monchoux, Ph.D. Thesis, Institut National des Sciences Appliquées, Lyon, France, 2000.
[4] A. Suzuki, Y. Hirose, Z. Yajima, K. Tanaka, Soc. Strength Fract. Mater. 27 (1993) 9–21.
[5] Y. Nadot, J. Mendez, N. Ranganathian, Fatigue Fract. Eng. Mater. Struct. 22 (1999) 289–300.
[6] K. Tokaji, T. Ogawa, Mater. Sci. Res. Int. 2 (1996) 39–45.
[7] H. Yaacoub, A. Agha, S. Beranger, R. Billardon, Fatigue Fract. Eng. Mater. Struct. 21 (1998) 287–296.
[8] E. Maire, J.Y. Buffiere, L. Salvo, J.J. Blandin, W. Ludwig, J.M. Letang, Adv. Eng. Mater. 3 (2001) 539–546.
[9] T.J. Marrow, J.Y. Buffiere, P.J. Withers, G. Johnson, D. Engelberg, Int. J. Fatigue 26 (2004) 717–725.
[10] P. Dierickx, Ph.D. Thesis, Institut National des Sciences Appliquées, Lyon, France, 1996.
[11] R.E. Peterson, Stress Concentration Factors, Wiley-Interscience, New York, 1973.
[12] A. Borbely, H. Mughrabi, G. Eisenmeier, H.W. Höppel, Int. J. Fract. 115 (2002) 227–232.
[13] J.Y. Buffière, S. Savelli, P.H. Jouneau, E. Maire, R. Fougères, Mater. Sci. Eng. A316 (2001) 115–126.